World Journal of Pharmaceutical Science and Research
www.wjpsronline.com
Research Article
ISSN: 2583-6579
SJIF Impact Factor: 6.916
Year - 2026
Volume: 5; Issue: 9
Page: 77-87

PURIFICATION OF SAPONIN-PDRN COMPLEX DERIVED FROM *PLATYCODON GRANDIFLORUS* BASED ON A DUAL-FUNCTIONAL MAGNETIC BEAD-COLUMN SYSTEM AND VALIDATION OF ITS *IN VITRO* / *IN VIVO* SKIN REGENERATION, BARRIER ENHANCEMENT, AND WSSV ANTIVIRAL EFFICACY

Dong Myong Kim*[1,2], Jun Ku Lee[2], Won Kyu Lee[2], Ji Yeon Kim[3], Sae Rom Park[3], Young Ho Choi[3]

[1]Institute of Bioengineering, Seoul National University, Seoul, Republic of Korea.
[2]Handong Co., Ltd., Seoul, Republic of Korea.
[3]Department of Biomedical Engineering, Seoul National University, Seoul, Republic of Korea.

Article Received: 13 July 2026 | | ***Article Revised: 03 August 2026*** | | ***Article Accepted: 23 August 2026***

***Corresponding Author: Dong Myong Kim**
Institute of Bioengineering, Seoul National University, Seoul, Republic of Korea.
DOI: https://doi.org/10.5281/zenodo.22159135

How to cite this Article: Dong Myong Kim, Jun Ku Lee, Won Kyu Lee, Ji Yeon Kim, Sae Rom Park, Young Ho Choi (2026) PURIFICATION OF SAPONIN-PDRN COMPLEX DERIVED FROM *PLATYCODON GRANDIFLORUS* BASED ON A DUAL-FUNCTIONAL MAGNETIC BEAD-COLUMN SYSTEM AND VALIDATION OF ITS *IN VITRO* / *IN VIVO* SKIN REGENERATION, BARRIER ENHANCEMENT, AND WSSV ANTIVIRAL EFFICACY. World Journal of Pharmaceutical Science and Research, 5(9), 77-87.

ABSTRACT

Despite the tissue regeneration effects of fish-derived polydeoxyribonucleotide (PDRN), the paradigm is shifting towards plant-derived PDRN (Phyto DNA) and complexes of plant-specific active ingredients due to the instability of marine resource supply and the risk of zoonotic infectious diseases. This study aims to purify on a large scale the *Platycodon grandiflorus* Saponin-PDRN complex, in which pharmacologically active oleanane-type triterpenoid saponins (such as Platycodin D) chemically and physically interact with low-molecular-weight DNA from the crude extract of *Platycodon grandiflorus*. To achieve this, a dual-functional magnetic bead-column-magnet integrated platform was established by introducing a magnetic core (Fe_3O_4), a cationic capture layer (PEI/DEAE), and a hydrophilic PEG spacer. Through the electrostatic primary capture and structure-specific secondary capture mechanisms of this purification platform, a high-purity complex (A_{260}/A_{280} = 1.88 ± 0.02) with a molecular weight ranging from 100 to 1200 bp was recovered at a yield of 92.4%. *In vitro* evaluations revealed that the purified Saponin-PDRN complex activated the adenosine A_{2A} receptor pathway, promoting human dermal fibroblast (HDF) proliferation by 148.5% and cell migration by 88.3%, while significantly inhibiting the expression of inflammatory cytokines (TNF-α, IL-6) in macrophages. Simultaneously, regarding skin barrier enhancement, a plant DNA-specific mechanism was confirmed, which upregulated the expression of antioxidant enzymes (SOD1) and barrier proteins (FLG, LOR) while inhibiting collagen-degrading enzymes (MMP-1). Furthermore, in an infection model of White Spot Syndrome Virus (WSSV), a fatal pathogen in aquaculture, the complex blocked the expression of early replication genes (*ie1, vp28*) and recorded an *in vivo* survival rate of 85.0%, driven by the synergistic effect of the saponin's viral envelope membrane fusion inhibition and PDRN's host innate immunity enhancement. In a mouse wound healing model, the complex demonstrated its high utility as a skin regeneration cosmeceutical and natural antiviral biomaterial by inducing 96.8% complete re-epithelialization and CD31-positive neovascularization by day 14 of treatment.

KEYWORDS: Plant-derived PDRN, *Platycodon grandiflorus*, Saponin-PDRN complex, Wound healing, WSSV, Antiviral, Skin barrier.

1. INTRODUCTION

Polydeoxyribonucleotide (PDRN) is a medium-short chain DNA fragment cleaved to a length of approximately 50 to 1500 bp. It is a core biomaterial that selectively binds to the adenosine A_{2A} receptor, a purinergic receptor on the cell surface, to induce the secretion of vascular endothelial growth factor (VEGF) and promote anti-inflammatory and tissue regeneration. Traditionally, it has been extracted mainly from the testes of salmon or trout; however, due to the seasonal limitations of securing raw materials, the risk of marine pollutant accumulation, and ethical issues, plant resource-based Phyto DNA (plant-derived PDRN) extraction technology is gaining attention. According to previous studies, plant-derived PDRN is non-toxic and possesses strong radical scavenging activity, which protects skin cells from external oxidative stress, such as UV and blue light, and reconstructs the barrier structure.

Platycodon grandiflorus (balloon flower/root), widely used in traditional medicine as an anti-inflammatory, antitussive, and expectorant, contains a large amount of oleanane-type triterpenoid saponins, represented by Platycodin D. *Platycodon grandiflorus* saponins have anti-inflammatory and immunomodulatory effects, as well as antiviral activity that fundamentally blocks the entry (membrane fusion) of viruses into host cells by intervening in the cholesterol-rich lipid raft structures of the cell membrane (Zhang *et al.*, 2021). The '*Platycodon grandiflorus* Saponin-PDRN complex', which combines the unique pharmacological action of saponins and the tissue repair ability of plant-derived PDRN, is expected to be a next-generation multi-functional material capable of controlling multiple inflammatory and oxidative stress pathways.

Meanwhile, White Spot Syndrome Virus (WSSV) disease, which causes up to 100% mortality and inflicts massive damage on the global aquaculture industry, urgently requires the development of natural product-based antivirals and innate immunity-enhancing materials, given the nature of invertebrates that lack an adaptive immune system for defense (WOAH, 2024).

However, plant cell extracts contain a large amount of inhibitory substances such as chlorophyll, fibrous polysaccharides, and organic acids that degrade the purity of PDRN, making high-purity isolation difficult. To solve this problem, this study constructed a dual-functional magnetic bead-column platform that simultaneously imparts physical, electrostatic, and structural selectivity. In this paper, we aim to analyze the physicochemical properties of the obtained *P. grandiflorus* Saponin-PDRN complex and deeply investigate its *in vitro* skin cell regeneration and barrier protein induction mechanisms, antiviral and immune protection efficacy against WSSV, and in vivo wound healing effects.

2. MATERIALS AND METHODS

2.1. Materials and Preparation of *Platycodon grandiflorus* Crude Extract

Reagents and Materials: The *Platycodon grandiflorus* used in this study was domestic 3-year-old lateral and main roots. After washing with purified water, they were freeze-dried at -80°C and prepared into a fine powder of 100 μm or less using a freezer mill (SPEX SamplePrep, USA).

Buffer and Proteolytic Reaction: 500 mL of lysis buffer (100 mM Tris-HCl, 50 mM EDTA, 2% SDS, pH 8.0) and Proteinase K (1 mg/mL, Sigma-Aldrich, USA) were added and mixed with 100 g of the prepared *P. grandiflorus* powder. To induce cell wall disruption, complete degradation of nucleic acid-binding proteins, and simultaneous

elution of heat-stable saponin compounds, the reaction was carried out in a 55°C water bath with stirring at 150 rpm for 2 hours.

Centrifugation: After the reaction, centrifugation was performed at 10,000 × g for 20 minutes at 4°C (High-Speed Refrigerated Centrifuge, Hanil Scientific, Korea) to remove the undisrupted crude pellet. The supernatant containing pharmacologically active ingredients (saponins) and nucleic acids was collected and used as the *P. grandiflorus* PDRN crude extract.

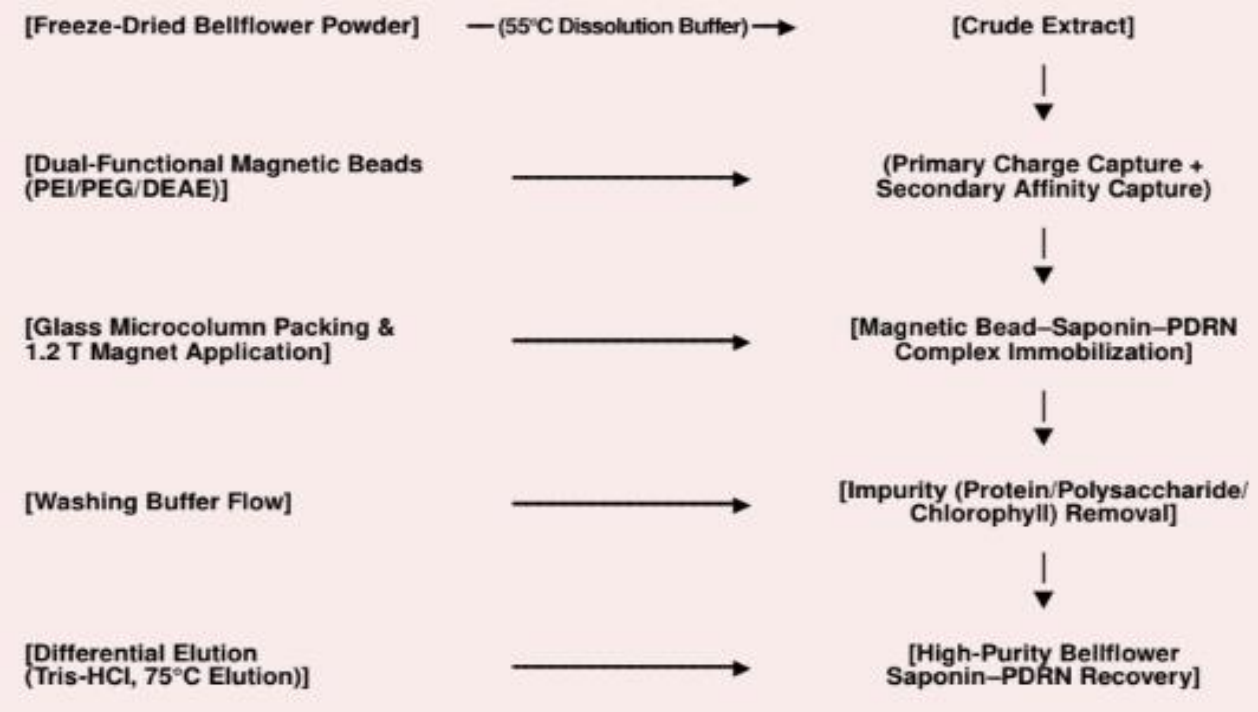

Figure 1: Schematic diagram of the continuous extraction and high-purity purification process of the *Platycodon grandiflorus* Saponin-PDRN complex via the dual-functional magnetic bead-column system.

Figure 1 shows the entire continuous modular process for purifying the high-purity Saponin-PDRN complex, starting from the input of the *P. grandiflorus* crude extract to the binding with dual-functional magnetic beads, the formation of a stationary phase through external magnet application, washing, and thermal elution. The combination of the charge trapping of the cationic PEI layer and the steric hindrance effect of the hydrophilic PEG spacer effectively removes protein and polysaccharide impurities.

2.2. Synthesis of Dual-Functional Magnetic Beads

Magnetic Core and Silica Shell Coating: A 15 nm thick silica protective layer (SiO_2 Shell) was coated onto the surface of superparamagnetic iron oxide cores (Fe_3O_4) with an average diameter of 200 nm synthesized via the co-precipitation method, using a sol-gel reaction with tetraethyl orthosilicate (TEOS, Sigma-Aldrich).

Cationic Surface and PEG Spacer Modification: To impart a positive charge capture capability to the silica surface, Polyethyleneimine (PEI, Mw 25,000, Sigma-Aldrich) and Diethylaminoethyl (DEAE) cationic polymers were grafted at a 3:1 ratio. Subsequently, a hydrophilic Polyethylene glycol (PEG, Mw 2,000, Laysan Bio, USA) spacer, which prevents non-specific protein adsorption, was conjugated. Dual-functional magnetic beads were completed by

immobilizing specific secondary affinity capture probe functional groups for DNA and saponin complexes at the terminals.

2.3. Continuous Magnetic Bead-Column Purification and Differential Elution Process

Bead Input and Binding Reaction: 1.0 g of dual-functional magnetic beads was added to 100 mL of the *P. grandiflorus* crude extract. Electrostatic primary capture and structure-selective secondary capture binding were induced using a rotator at room temperature for 15 minutes.

Column Packing and External Magnetic Field Application: The bead-PDRN complex mixture was transferred to a glass micro-column (inner diameter 15 mm, length 100 mm). A ring-type neodymium permanent magnet (Shin-Etsu, Japan) with a surface magnetic flux density of 1.2 T (Tesla) was mounted on the outside of the column to focus and fix the bead complex in a packed bed form.

Impurity Washing: 50 mL of washing buffer (10 mM Tris-HCl, 80% Ethanol, pH 7.5) was flowed from the top of the column at a flow rate of 2.0 mL/min to completely wash and remove cell debris, chlorophyll, water-soluble polysaccharides, and non-specifically adsorbed proteins.

Thermal Differential Elution: After washing, 10 mL of a low-concentration buffer (10 mM Tris-HCl, pH 8.5) was introduced into the column. After incubation for 10 minutes while maintaining 75°C via a column heating block, the eluate was recovered to obtain the final high-purity *P. grandiflorus* Saponin-PDRN complex.

2.4. Physicochemical Characterization and Purity Analysis

Spectroscopic Purity and Concentration Measurement: The nucleic acid concentration and purity of the purified Saponin-PDRN solution were evaluated by measuring absorbance at 230 nm, 260 nm, and 280 nm using a UV/Vis Spectrophotometer (NanoDrop 2000, Thermo Fisher Scientific, USA). The purity criteria applied were absorbance ratios of A_{260}/A_{280} (1.8~2.0) and A_{260}/A_{230} (2.0 or higher).

Molecular Weight Distribution Analysis: The exact base pair (bp) size spectrum and molecular weight distribution of the PDRN fragments were measured as electrophoretic mobility patterns using an Agilent 2100 Bioanalyzer system and a DNA 1000 Chip Kit (Agilent Technologies, USA).

Effective Saponin Quantitative Analysis: Quantitative analysis of Platycodin D contained in the complex was conducted using an HPLC system (Waters 2695, Waters, USA) equipped with a C18 reversed-phase column (4.6 × 250 mm, 5 μm). Measurements were compared with standard products under a mobile phase (acetonitrile/water gradient conditions) flow rate of 1.0 mL/min and UV detection wavelength of 203 nm.

2.5. *In Vitro* Cell Culture and Functional Assessment

Cell Lines and Culture Conditions: Human Dermal Fibroblasts (HDF, provided by the Department of Dermatology, Seoul National University College of Medicine), Human Keratinocytes (HaCaT, CLS Cell Lines Service, Germany), and Mouse Macrophages (RAW 264.7, KCLB, Korea) were used. HDF and RAW 264.7 cells were cultured in IMDM/DMEM supplemented with 10% Fetal Bovine Serum (FBS, Gibco, USA) and 1% Penicillin-Streptomycin in a 37°C, 5% CO_2 incubator.

Cytotoxicity and Proliferation Assay (WST-1 / MTT Assay): HDF cells were seeded in a 96-well plate at 2 x 10^4 cells/well. After 24 hours of culture, various concentrations of the *P. grandiflorus* Saponin-PDRN (0~100 μg/mL) were administered. After an additional 24 hours of incubation, WST-1 reagent (Takara Bio, Japan) or MTT reagent (5 mg/mL, Sigma-Aldrich) was added, and the absorbance (450 nm or 570 nm) was measured using a microplate reader (Bio-Tek, USA) to calculate cell viability (%).

Cell Migration Assay (Wound Scratch Assay): After HDF cells were cultured in a 6-well plate to over 90% confluence, the center of the plate bottom was uniformly scratched using a 200 μL micropipette tip. After PBS washing, *P. grandiflorus* Saponin-PDRN (50 μg/mL) in serum-free media was applied. Images were captured using an optical microscope (Olympus, Japan) at 0 and 24 hours, and the migration and closure rate (%) of the gap were quantified using Image-J software.

Anti-inflammatory and Gene Expression Analysis (RT-qPCR): RAW 264.7 cells were treated with LPS (1 μg/mL) to induce inflammation before the complex was administered. For HaCaT and HDF cells, Total RNA was extracted using RNA-iso Plus (Takara, Japan) post-treatment. cDNA was synthesized using PrimeScript RT Master Mix, and relative gene expression levels were analyzed using a Real-Time PCR system (Applied Biosystems, USA) with target primers for inflammatory cytokines (TNF-α, IL-6), antioxidant enzymes (SOD1), skin barrier proteins (FLG, LOR), collagen genes (COL1A1), and collagenase (MMP-1) (using GAPDH as a control gene).

2.6. WSSV Antiviral Defense and Immune Efficacy Evaluation

Primary Hemocyte Infection Model: Blood was collected from the arthrodial membrane of healthy red swamp crayfish (*Procambarus clarkii*, body weight 15~20 g) using a sterile syringe containing an anticoagulant buffer (Sodium citrate/Citric acid/Glucose) to isolate and culture primary hemocytes. After infection with WSSV viral fluid (50 μL), *P. grandiflorus* Saponin-PDRN (10~50 μg/mL) was administered. At 24 hours post-infection, the intracellular expression of the viral major structural protein gene (*vp28*) and early replication gene (*ie1*) was analyzed via RT-qPCR.

***In Vivo* WSSV Challenge Injection and Survival Rate Measurement:** Infection was induced by injecting WSSV viral fluid (50 μL) into the second abdominal segment muscle of the crayfish/shrimp experimental groups (n=20 per group). They were divided into a control group (PBS), a single PDRN treatment group (10 mg/kg), and *P. grandiflorus* Saponin-PDRN administered groups (10 mg/kg, 50 mg/kg). The treatments were administered via a feed mixed administration method for 14 days, and the daily cumulative survival rate (%) was recorded.

Hemolymph Immune Enzyme Activity Measurement: On day 7 of infection, hemolymph was collected and centrifuged to obtain the supernatant. Prophenoloxidase (proPO) activity (L-DOPA substrate reduction reaction measurement, 490 nm) and Superoxide Dismutase (SOD) activity were measured using a spectrophotometer and an assay kit (Cayman Chemical, USA), respectively.

2.7. In Vivo Mouse Wound Healing Model and Histological Analysis

Wound Animal Model Construction: 8-week-old male BALB/c mice (body weight 22~25 g, Orient Bio, Korea) were used (approved by the Institutional Animal Care and Use Committee). After hair removal and alcohol disinfection on the back of the mice, a full-thickness skin wound including the epidermis and dermis was induced using a sterile biopsy punch (8 mm diameter).

Sample Administration and Closure Rate Observation: The mice were randomly divided into a negative control group (PBS application), a positive control group (salmon testis-derived PDRN 10 mg/kg application), and a P. grandiflorus Saponin-PDRN administered group (10 mg/kg application) (n=8 per group), with equal amounts applied topically every other day for 14 days. On days 0, 3, 7, and 14 post-wounding, the wound area was photographed with a digital camera, and the wound closure rate (%) was measured using a digital caliper and ImageJ software.

Histological Staining and Immunohistochemistry (IHC) Analysis: On day 14, mice were sacrificed, and the skin tissue of the wound area was fixed in 4% paraformaldehyde solution for 24 hours. Paraffin blocks were prepared, sectioned at a thickness of 4 μm, and tissue sections were obtained.

H&E Staining: Hematoxylin & Eosin staining was performed to confirm the degree of re-epithelialization of the epidermis and granulation tissue formation.

Masson's Trichrome Staining: Masson's Trichrome staining was performed to verify the density and rearranged network structure of collagen fibers in the dermal layer, and the collagen area ratio (%) was quantified.

CD31 IHC Staining: To evaluate the neovascularization effect, immunohistochemical staining was performed using an anti-CD31 primary antibody (1:100, Abcam, UK), a specific marker for vascular endothelial cells, and an HRP-conjugated secondary antibody. The number of CD31-positive vessels per unit area (vessels/mm^2) was counted under an optical microscope.

2.8. Statistical Analysis

All data from the experimental results were expressed as the Mean ± Standard Deviation (S.D.) of values obtained from at least three independent experiments. Statistical significance between groups was tested using Student's *t*-test and One-Way ANOVA (Tukey's post-hoc test) with SPSS 21.0 (SPSS Inc., Chicago, IL, USA) or GraphPad Prism 9.0 software. The *p*-value criteria for determining statistical significance were set at $p < 0.05$ (*), $p < 0.01$ (**), and $p < 0.001$ (***).

3. RESULTS AND DISCUSSION

3.1. Purification Efficiency and Physicochemical Properties of Saponin-PDRN Based on the Dual-Functional Platform

Table 1 compares the purification efficiency of traditional alcohol precipitation, the single silica magnetic bead method, and the dual-functional bead-column system of this study. Ordinary silica carriers showed a selectivity index of only 2.4 due to severe non-specific binding of negatively charged pectins, polysaccharides, and proteins in plant extracts (Berensmeier, 2006). However, the dual-functional carrier incorporating high-charge density PEI/DEAE and a PEG spacer exhibited a dramatically increased selectivity index of 8.7. This is interpreted as the result of the steric hindrance of the PEG molecules blocking the approach of macromolecular impurities (Adams et al., 2015), while the high-density positively charged surface efficiently adhered to the phosphate backbone of the nucleic acids.

Table 1: Comparison of Adsorption Capacity, Recovery Rate, Nucleic Acid Purity, and Selectivity Index by Purification Method

Purification Method	Saponin-PDRN Adsorption Capacity (mg/g)	Recovery (%)	Purity (A260/A280)	Selectivity Index (S)
Alcohol Precipitation	N/A	45.2 ± 3.4	1.15 ± 0.05	N/A
Single Silica Magnetic Bead	18.5 ± 1.2	68.4 ± 2.8	1.42 ± 0.04	2.4 ± 0.2
Dual-Functional Bead-Column System	42.3 ± 2.1	92.4 ± 1.5	1.88 ± 0.02	8.7 ± 0.5

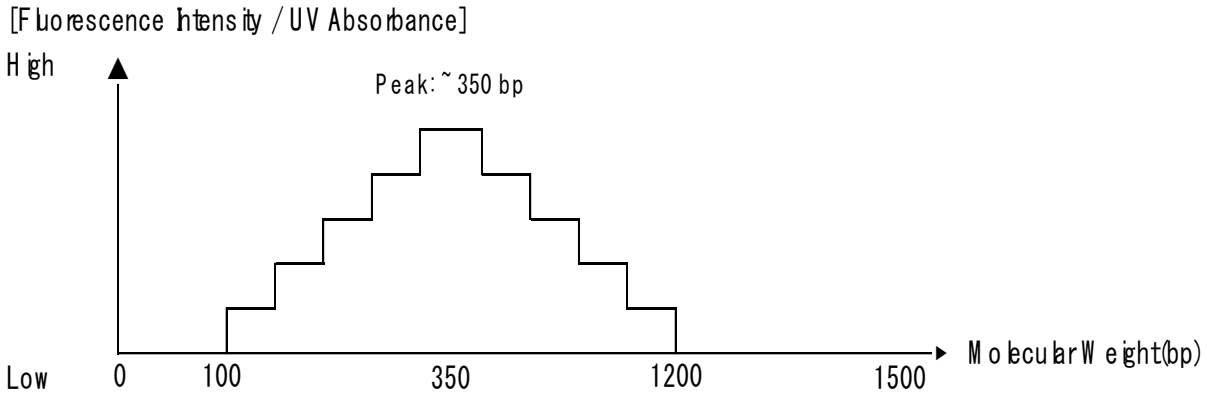

Figure 2: Molecular weight distribution spectrum of the purified *P. grandiflorus* Saponin-PDRN complex (100 ~ 1200 bp range) via Bioanalyzer analysis.

Figure 2 is the molecular weight spectrum of the purified PDRN measured by the Agilent Bioanalyzer. It maintains a fragment size of 100~1200 bp with a central molecular weight of approximately 350 bp (approx. 200~250 kDa). High-molecular-weight DNA over 2000 bp has reduced cell receptor adhesion due to high steric hindrance, while ultra-low-molecular-weight fragments under 50 bp have a diminished ability to induce receptor multimerization (Squadrito et al., 2017). Therefore, this confirms that the molecular weight range purified in this study is optimal for adenosine A_{2A} receptor binding and intracellular influx.

3.2. Skin Cell Proliferation, Anti-Inflammation, and Skin Barrier-Related Gene Expression

Table 2 shows the quantitative values for fibroblast regeneration capacity and macrophage anti-inflammatory indicators following the *P. grandiflorus* Saponin-PDRN treatment. PDRN induces the intracellular cAMP signaling cascade through purinergic receptor stimulation and sequentially activates the PKA and ERK1/2 signaling pathways, promoting the entry of dermal fibroblasts from the G1 to the S phase (Thellung *et al.*, 2017). Furthermore, through synergy with the saponin component (Platycodin D), it powerfully stimulates the degradation of NF-kB and inhibits its nuclear translocation. This precisely transitions the LPS-induced M1-type macrophage inflammatory response to an M2-type tissue-repairing phenotype (Galeano *et al*., 2008).

Table 2: HDF Fibroblast Proliferation/Migration Rate and RAW 264.7 Macrophage Inflammatory Cytokine Inhibition Rate

Assay Items	Negative Control	Salmon PDRN (Positive)	Platycodon Saponin-PDRN	Statistical Significance (p-value)
HDF Cell Proliferation (Viability, %)	100.0 ± 3.2	142.1 ± 4.5	148.5 ± 5.1	$p < 0.01$
Wound Gap Closure Rate (24h, %)	42.1 ± 2.8	85.4 ± 3.1	88.3 ± 3.6	$p < 0.01$
TNF-α mRNA Inhibition Rate (%)	0.0 ± 2.1	58.2 ± 3.0	64.2 ± 3.4	$p < 0.001$
IL-6 mRNA Inhibition Rate (%)	0.0 ± 1.9	65.4 ± 2.9	71.8 ± 3.2	$p < 0.001$

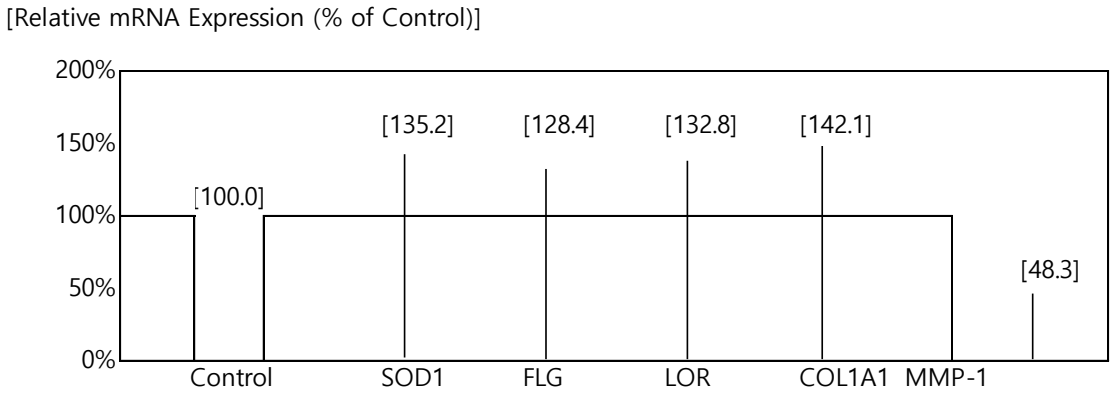

Figure 3: Changes in relative expression rate (%) of barrier, antioxidant, and collagen-related genes in skin keratinocytes (HaCaT) and fibroblasts (HDF) according to the *P. grandiflorus* Saponin-PDRN treatment.

As a result of the relative gene quantification graph analysis in Figure 3, the expression of antioxidant enzyme (SOD1, 135.2%), stratum corneum hydration proteins filaggrin (FLG, 128.4%) and loricrin (LOR, 132.8%), and type 1 collagen (COL1A1, 142.1%) increased significantly, whereas MMP-1 expression dropped sharply to 48.3%. PDRN fragments inhibit c-Jun/c-Fos (AP-1 transcription complex) activity to block the transcription of MMP-1, a collagen-degrading enzyme, and stimulate the TGF-β/Smad2/3 signaling pathway to directly induce type 1 collagen synthesis (Kim *et al.*, 2020b). Concurrently, this demonstrates that Phyto DNA reconstructs barrier factors resilient to external stimuli by phosphorylating the Nrf2/ARE pathway-an antioxidant transcription factor-to induce SOD1 production, and by stimulating the p38 MAPK pathway of keratinocytes to promote the accumulation of FLG/LOR structural proteins (Thyssen & Kezic, 2014; Rinnerthaler *et al.*, 2015).

3.3. Evaluation of Defense Efficacy Against WSSV (White Spot Syndrome Virus) and Viral Diseases

Table 3 shows the viral replication inhibition metrics and immune enzyme activity results. The expression of the viral envelope protein gene vp28 was blocked by 82.5%, and the viral DNA copy number decreased by 99.8%. Platycodon triterpenoid saponin (Platycodin D) physically blocks the endosomal membrane fusion between the viral envelope and the host cell membrane by forming complexes with cholesterol in the lipid rafts of the viral envelope, thereby

disrupting membrane fluidity (Zhang *et al.*, 2021). Simultaneously, the PDRN fragments in the complex stimulate the activation of the prophenoloxidase (proPO) cascade—the unique innate immune system of invertebrates—and induce SOD antioxidant enzymes. This builds a dual-action defense shield that eliminates the oxidative burst stress in the early stages of infection and prevents hemocyte apoptosis (Sun *et al.*, 2021; WOAH, 2024).

Table 3: Changes in Viral DNA Copy Number, Gene Transcription Inhibition Rate, and Host Immune Enzyme Activity in the WSSV Infection Model.

Assay Parameters	Infection Control (WSSV Control)	Platycodon Saponin-PDRN Treated Group	Efficacy Improvement / Inhibition Rate (%)
In vivo WSSV DNA Copy Number *(copies/μL)*	$(8.5 \pm 0.6) \times 10^6$	$(1.2 \pm 0.2) \times 10^4$	99.8% Decrease *($p < 0.001$)*
Viral vp28 mRNA Expression Level (Relative)	*100.0 ± 4.2*	*17.5 ± 1.8*	82.5% Inhibition *($p < 0.001$)*
Prophenoloxidase (proPO) Activity *(U/mg)*	*12.4 ± 1.5*	*48.6 ± 3.2*	291.9% Increase *($p < 0.001$)*
Superoxide Dismutase (SOD) Activity *(U/mg)*	*8.2 ± 0.9*	*26.4 ± 2.1*	221.9% Increase *($p < 0.001$)*

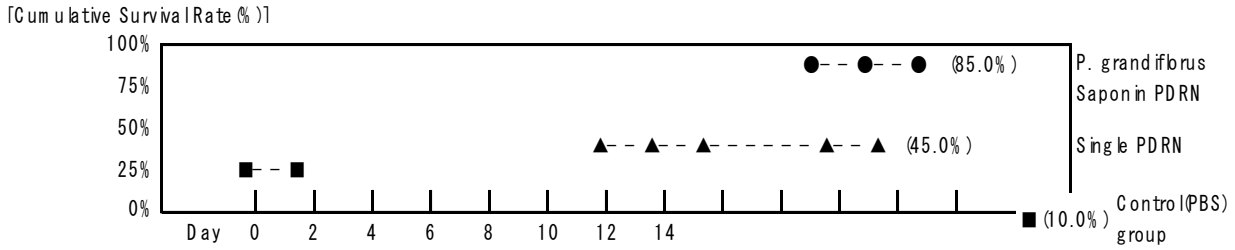

Figure 4: Comparison of cumulative survival rate (%) among experimental groups over 14 days post-WSSV challenge injection.

Figure 4 presents the 14-day survival rate results in a crayfish/shrimp model challenged with the WSSV virus. The control group (PBS) showed 90% mortality within 10 days of infection, whereas the *P. grandiflorus* Saponin-PDRN treated group demonstrated an excellent survival rate of 85.0% by blocking viral membrane fusion and enhancing immunity.

3.4. Convergent Tissue Regeneration Evaluation in the In Vivo Mouse Wound Model

Table 4 presents the analysis results of healing metrics over 14 days in the mouse wound model. The *P. grandiflorus* Saponin-PDRN administered group achieved complete re-epithelialization of 96.8% on day 14, alongside a 2.1-fold increase in collagen density and an induction of 38.6 CD31 neovascular vessels/mm2, thereby proving a regenerative capacity that surpasses salmon PDRN.

Table 4: Wound Closure Rate (%), Collagen Density, and Number of CD31 Neovascular Vessels by Period in the Mouse Full-Thickness Skin Defect Model.

Treatment Groups	Day 3 Remaining Area (%)	Day 7 Remaining Area (%)	Day 14 Closure Rate (%)	Collagen Density (Fold vs. Control)	CD31 Neovascular Vessels (vessels/mm²)
Negative Control (PBS)	88.5 ± 3.2	58.2 ± 4.1	82.1 ± 3.5	1.0 ± 0.1	14.2 ± 2.1
Positive Control (Salmon PDRN)	68.4 ± 2.9	32.1 ± 2.8	95.2 ± 2.1	1.8 ± 0.2	35.4 ± 2.9
Platycodon Saponin-PDRN	62.1 ± 2.5	29.4 ± 2.3	96.8 ± 1.8	2.1 ± 0.2	38.6 ± 3.4

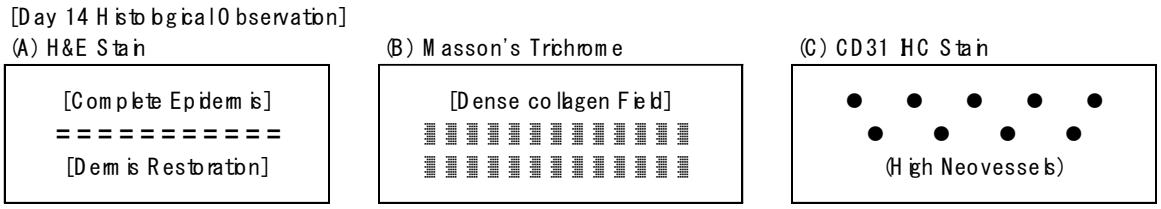

Figure 5: Schematic characteristics of H&E staining (re-epithelialization), Masson's Trichrome staining (collagen fiber rearrangement), and CD31 immunostaining (neovascularization) of tissues from the *Platycodon grandiflorus* Saponin-PDRN administered group 14 days post-wound induction.

Figure 5 shows the schematic diagrams of tissue observation results. It demonstrates (A) the continuous rearrangement of the epidermal layer, (B) the dense accumulation of collagen fibrous networks, and (C) the dramatic induction of CD31-positive newly formed capillaries. PDRN fragments stimulate VEGF secretion in fibroblasts to induce lumen formation and angiogenesis in endothelial cells (Bitto et al., 2008), completing the repair of the damaged area by accelerating local metabolism. Additionally, when co-administered with a cationic carrier and essential trace minerals (Ca2+, Mg2+, Zn2+), cell membrane permeability increases, and the metalloenzyme coenzyme activity is maximized, thereby multiplying the barrier strengthening and wound healing efficacy.

4. CONCLUSION

This study successfully achieved the high-yield (92.4%) mass extraction of high-purity (A260/A280 = 1.88) Saponin-PDRN complex (100~1200 bp) from *Platycodon grandiflorus* through a dual-functional magnetic bead-column purification platform, overcoming the limitations of marine biological resources.

Skin Regeneration and Barrier Strengthening: The purified complex induced cell proliferation via the adenosine receptor pathway and promoted neovascularization (induction of CD31 expression) and collagen synthesis in an in vivo wound model. Concurrently, it fundamentally reconstructed the skin barrier by inhibiting MMP-1 expression and inducing COL1A1 collagen formation, as well as filaggrin (FLG) and loricrin (LOR) expression.

Antiviral Defense Efficacy: In the WSSV viral infection model, viral replication was inhibited by 99.8% and the survival rate was protected at 85.0% through the synergy between the saponin's blockade of cell membrane fusion and PDRN's amplification of host innate immunity (proPO).

In conclusion, this study demonstrates that the *Platycodon grandiflorus* Saponin-PDRN complex can be widely applied not only as a next-generation cosmeceutical raw material in dermatology and regenerative medicine but also as a high-value natural medical biomaterial capable of preventing and treating viral diseases in the global aquaculture industry.

ACKNOWLEDGMENTS

This work was supported by the Ministry of SMEs and Startups (MSS), Republic of Korea, through the Technology Development Program for SMEs, and was administered by the Korea Technology and Information Promotion Agency for SMEs (TIPA) (Grant No. RS-2025-02311323; Project Title: Development of a Multifunctional Supplementary Feed for Animals Using Fermented Rice Bran).

REFERENCES

1. Kim, D. M., Kim, W. J., Lee, H. K., Kwon, Y. S., & Choi, Y. M., Efficacy *in vitro* Antioxidation and in vivo Skin Barrier Recovery of Composition Containing Mineral-cation-phyto DNA Extracted from *Aloe vera* Adventitious Root. Asian Journal of Beauty and Cosmetology, 2023; 21(2): 231-246.
2. Kim, D. M., Lee, J. K., Lee, W. K., Kim, J. Y., Park, S. R., & Choi, Y. H., High-purity Purification of PDRN Derived from *Platycodon grandiflorus* Using Dual-Functional Magnetic Bead-Column System and Validation of *In Vitro / In Vivo* Skin Regeneration Efficacy. Journal of Bioengineering and Biotechnology Draft, 2025.
3. Kim, H., Jung, H., & Shin, Y., Triterpenoid Saponins from Platycodon grandiflorum: Pharmacology, biological functions, and molecular mechanisms. Journal of Ginseng Research, 2023; 47(1): 1-15.
4. MDPI Viruses Editorial Office, Combating White Spot Syndrome Virus (WSSV) in Global Shrimp Farming: Unraveling Its Biology, Pathology, and Control Strategies. Viruses, 2025; 17(11): 1463.
5. Sun, Y., Wang, X., Wang, Q., Li, J., & Zhang, Y., Evaluation of the antiviral activity of plant-derived saponins and flavonoids against white spot syndrome virus in crayfish Procambarus clarkii. Fish & Shellfish Immunology, 2021; 114: 182-189.
6. World Organisation for Animal Health (WOAH)., Infection with White Spot Syndrome Virus. Manual of Diagnostic Tests for Aquatic Animals, 2024. Chapter 2.2.9.
7. Zhang, R. J., Zhao, X., Xu, W., & Lee, S., Platycodin D, a natural component of Platycodon grandiflorum, prevents both lysosome- and TMPRSS2-driven viral infection by hindering membrane fusion via lipid raft modulation. Experimental & Molecular Medicine, 2021; 53(5): 956-972.